Island-size distribution and capture numbers in three-dimensional nucleation: Comparison with mean-field behavior

Feng Shi,* Yunsic Shim,† and Jacques G. Amar‡
Department of Physics & Astronomy, University of Toledo, Toledo, Ohio 43606, USA
(Received 4 February 2005; published 21 June 2005)

The scaling of the monomer and island densities, island-size distribution (ISD), capture-number distribution (CND), and capture-zone distribution is studied as a function of the fraction of occupied sites (coverage) and ratio D/F of the monomer hopping rate D to the (per site) monomer creation rate F in a three-dimensional (3D) point-island model of irreversible nucleation and island growth. Our model is a 3D analog of submonolayer growth and may also be viewed as a simplified model of the early stages of vacancy cluster nucleation and growth under irradiation. Good agreement is found between mean-field (MF) rate-equation results for the average island and monomer densities and our simulation results. In addition, due to the decreased influence of correlations and fluctuations in 3D, the scaled CND depends only weakly on the island-size. As a result, the scaled ISD is significantly sharper than obtained in 2D and diverges with increasing D/F. However, for large D/F both the scaled ISD and the scaled CND differ from the MF prediction. In particular, the scaled ISD diverges more slowly than the MF prediction while the asymptotic divergence occurs at a value of the scaled island size which is larger than the MF prediction. These results are further supported by an analysis of the asymptotic scaled capture-number distribution.

DOI: 10.1103/PhysRevB.71.245411 PACS number(s): 81.15.Aa, 68.55.Ac, 68.43.Jk

I. INTRODUCTION

Cluster nucleation and growth is the central feature of many physical processes. The nucleation and growth of islands in submonolayer epitaxial growth has been studied intensively both experimentally[1–10] and theoretically[11–30] since the structures formed in the submonolayer regime can strongly influence the morphology and properties of the resultant multilayer film. For example, recently considerable theoretical effort has been carried out towards an understanding of the scaling properties of the island-size distribution $N_s(\theta)$ (where N_s is the number of islands of size s at coverage θ) in submonolayer growth.[11–30] In the precoalescence regime the island-size distribution satisfies the scaling form[14,15]

$$N_s(\theta) = \frac{\theta}{S^2} f\left(\frac{s}{S}\right), \tag{1}$$

where S is the average island size and the scaling function $f(u)$ depends on the critical island size and island morphology.[18]

One of the standard tools used in these studies is the rate-equation (RE) approach.[11,12,31] In this approach the coverage dependence of the island-size distribution (ISD) is calculated through a set of deterministic reaction-diffusion equations which involve a set of rate coefficients usually called capture numbers.[11,12] For the irreversible growth of point islands, rate equations valid in the precoalescence regime may be written in the form

$$\frac{dN_1}{d\theta} = 1 - 2R\sigma_1 N_1^2 - RN_1 \sum_{s=2}^{\infty} \sigma_s N_s - \kappa_1 N_1 - \sum_{s=1}^{\infty} \kappa_s N_s, \tag{2}$$

$$\frac{dN_s}{d\theta} = R\sigma_{s-1} N_1 N_{s-1} - R\sigma_s N_1 N_s + \kappa_{s-1} N_{s-1} - \kappa_s N_s, \tag{3}$$

where the capture numbers σ_s (σ_1) correspond to the *average* capture rate of diffusing monomers by islands of size s (monomers), $R=D/F$ is the ratio of the monomer diffusion rate to the deposition rate, and the terms with κ_s ($\kappa_s=1$ for point islands) correspond to direct impingement. We note that the central problem in the RE approach is the determination of the size- and coverage-dependent capture numbers $\sigma_s(\theta)$.

The simplest possible assumption for the capture-number distribution (CND) is the mean-field assumption $\sigma_s(\theta)=\sigma_{av}$. While such an assumption may be adequate to describe the scaling of the average island density N and monomer density N_1 with coverage and D/F, it is not adequate to describe the ISD. For example, using two-dimensional (2D) kinetic Monte Carlo (KMC) simulations, Bartelt and Evans[19] showed that even for point islands there is a nontrivial dependence of the capture number on the island size due to the correlation between the island size and capture zone. In addition, they showed that in the asymptotic limit of large D/F, the scaled ISD is related to the scaled CND as

$$f(u) = f(0)\exp\left[\int_0^u dx \frac{2z - 1 - C'(x)}{C(x) - zx}\right], \tag{4}$$

where $C(s/S)=\sigma_s/\sigma_{av}$ is the scaled CND, z is the dynamical exponent describing the dependence of the average island size on coverage ($S \sim \theta^z$), and $f(0)$ is determined by the normalization condition $\int_0^\infty du\, f(u)=1$. We note that for irreversible growth of point islands as is considered here, one has $z=2/3$. As can be seen from Eq. (4), if $C(u)>zu$, then no divergence will occur. However, if $C(u)$ crosses zu at

some value u_c, then a divergence in the asymptotic ISD will occur if $C'(u_c) < 2z-1$.

This result highlights the importance of understanding the capture-number distribution in order to understand the scaling behavior of the ISD. For example, using this expression Bartelt and Evans were able to show[19] that the usual mean-field (MF) assumption that the capture number is independent of island size leads to a divergent ISD. On the other hand, by measuring the CND for various models in two-dimensional submonolayer island growth, they showed that due to correlations, the actual CND is not mean field but depends strongly on the island size. Accordingly, the scaled ISD for 2D nucleation and growth does not diverge in the asymptotic limit.

While the scaling behavior of the ISD and CND is now well understood for the case of two-dimensional nucleation and growth, the corresponding behavior has not been studied in three dimensions. This is of interest from a theoretical point of view, since we would like to understand to what extent fluctuations play a role in determining the scaled ISD and CND, and a comparison with 3D simulations would be quite useful in providing such understanding. In addition, the scaling behavior of the ISD in simple models of 3D nucleation and growth may also be important in understanding a variety of important processes. For example, the nucleation and growth of islands in bulk materials has attracted tremendous interest in recent years, as these processes create nanoparticles which as quantum dots are promising in fabricating light emission devices.[32–34]

Here we present results for the scaled island-size distribution and capture-number distribution obtained from KMC simulations of a simple point-island model of 3D nucleation and growth. For completeness, we also present the results of a self-consistent RE calculation which leads to good agreement with KMC simulations for the coverage dependence of the average island density $N(\theta)$ and monomer density $N_1(\theta)$. We find that, due to the decreased role of fluctuations and correlations in three dimensions, the scaled ISD in 3D is significantly sharper than in 2D and appears to diverge with increasing D/F, while the asymptotic CND depends only weakly on island size. However, the asymptotic scaled ISD and CND still appear to deviate from the MF prediction. We attribute this deviation to the existence of geometric effects and correlations which, although reduced in 3D, still appear to play a role in three dimensions.

This paper is organized as follows. In Sec. II we first describe our simulations and point-island model. In Sec. III we describe a self-consistent rate-equation approach to the calculation of the capture numbers. In Sec. IV we first present a comparison between our self-consistent RE results and KMC results for the average island and monomer densities. We then present our KMC results for the ISD and CND along with a comparison with the corresponding RE results. Results for the scaled capture-zone distribution (CZD) are also presented. Finally, we discuss and summarize our results in Sec. V.

II. MODEL AND SIMULATIONS

In order to study the scaling behavior of the ISD and CND in 3D nucleation and growth, we have studied a simple point-island model of irreversible nucleation and growth on a cubic lattice. Our model is a straightforward analog of the corresponding point-island model previously studied in two dimensions.[19] However, it may also be considered to be a simple model of vacancy cluster nucleation and growth in solids. We note that a more realistic model would take into account the increase of the lateral dimension of an island with island size. However, in the asymptotic limit of large D/F the point-island approximation is appropriate for extended islands up to a finite coverage ($\theta \leqslant 0.01$) since over this coverage range the average island separation is still significantly larger than the average island radius.[26]

In our model, monomers are randomly created throughout the lattice with creation rate F per site per unit time and then hop randomly in each of the six nearest-neighbor directions with hopping rate D_h. If a monomer lands on a site already occupied by another monomer or is created at such a site, then a dimer island is nucleated. Similarly, if a monomer lands on or is created at a site already occupied by an island, then that monomer is captured by that island and the island size increases by 1. As for 2D nucleation and growth the key parameter in this model is the ratio $R_h = D_h/F$ of the monomer hopping rate to the (per site) monomer creation rate or, equivalently, the ratio $R = D/F = R_h/6$.

In order to study the asymptotic scaling behavior, we have carried out simulations over a range of values of R_h ranging from 10^5 to 10^{10}. To avoid finite-size effects, simulations were carried out over a range of different values of the system size L ranging from $L=160$ to $L=450$. In addition, our results were typically averaged over 200 runs to obtain good statistics. For each set of parameters the scaled ISD, CND, and CZD were obtained for coverages up to $\theta=0.4$, while the average island density $N(\theta)$ and monomer density $N_1(\theta)$ were also measured. We note that in order to measure the capture-number distribution, the method outlined in Ref. 19 was used. In particular, the capture number $\sigma_s(\theta)$ was calculated using the expression $\sigma_s(\theta) = n_s^c/(R\Delta\theta N_1 N_s L^3)$ where n_s^c is the number of monomer capture events corresponding to an island of size s during a very small coverage interval ($\Delta\theta \simeq 0.001$). As in Ref. 19 the island size s at the beginning of the coverage interval was used when incrementing the counter n_s^c in order to obtain good statistics. We also note that in our capture-zone distribution calculations, the capture zone of an island was defined as corresponding to all monomer sites or empty sites which are closer to that island than any other island. If such a site was equally close to several islands, then that site's contribution to the capture zone was equally distributed between the islands.

III. SELF-CONSISTENT RATE-EQUATION CALCULATION

As in Ref. 17 we consider a quasistatic diffusion equation for the monomer density $n_1(r,\theta,\phi)$ surrounding an island of size s of the form

$$\nabla^2 n_1(r,\theta,\phi) - \xi^{-2}(n_1 - N_1) = 0, \tag{5}$$

where N_1 is the average monomer density and ξ corresponds to an overall average capture term. For consistency with the

RE's (2) and (3) we require $\xi^{-2}=2\sigma_1 N_1+\Sigma_{s=2}^{\infty}\sigma_s N_s$. We note that if we assume that $\sigma_s=\sigma_1=\sigma$, then this self-consistency condition may be written more simply as

$$\xi^{-2}=\sigma(N+2N_1). \tag{6}$$

Assuming spherical symmetry Eq. (5) may be written

$$\frac{1}{r^2}\frac{d}{dr}\left(r^2\frac{d\tilde{n}_1}{dr}\right)-\xi^{-2}\tilde{n}_1(r)=0, \tag{7}$$

where $\tilde{n}_1(r)=n_1(r)-N_1$. The general solution is given by

$$\tilde{n}_1(r)=A\frac{\sinh(r/\xi)}{r}+B\frac{\cosh(r/\xi)}{r}. \tag{8}$$

Using the boundary condition $n_1(R_s)=0$ (where R_s is the island radius) corresponding to irreversible growth, along with the asymptotic boundary condition $n_1(\infty)=N_1$, we obtain

$$n_1(r)=N_1[1-(R_s/r)e^{-(r-R_s)/\xi}]. \tag{9}$$

Equating the *microscopic* flux of atoms near the island $4\pi R_s^2 D[\partial n_1/\partial r]_{r=R_s}$ to the corresponding *macroscopic* RE-like term $DN_1\sigma_s$, we obtain, for the capture number,

$$\sigma_s=\frac{4\pi R_s^2}{N_1}\left(\frac{\partial n_1}{\partial r}\right)_{r=R_s}=4\pi R_s(1+R_s/\xi). \tag{10}$$

We note that this result agrees with that of Talbot and Willis[35] who carried out an analysis of the mean "sink" strength of voids in a random array of voids in an irradiated material.

For the point-island model the island radius R_s is independent of island size (i.e., $R_s=R_0$) which implies

$$\sigma_s=\sigma=4\pi R_0(1+R_0/\xi), \tag{11}$$

where R_0 is a model-dependent constant of order 1. Substituting the self-consistency condition (6) for ξ leads to the result

$$\sigma\simeq 4\pi R_0[1+\chi(1+\sqrt{1+2/\chi})], \tag{12}$$

where $\chi=(N+2N_1)2\pi R_0^3$ and $N=\Sigma_{s=2}^{\infty}N_s$ is the average island density. Using this result the contracted rate equations for the monomer and island densities may be written

$$\frac{dN_1}{d\theta}=1-2N_1-N-2(D/F)\sigma N_1^2-(D/F)\sigma N_1 N, \tag{13}$$

$$\frac{dN}{d\theta}=N_1+(D/F)\sigma N_1^2. \tag{14}$$

We note that for large D/F, Eq. (12) implies a capture number $\sigma\simeq 4\pi R_0$ which does not depend on coverage or D/F.

IV. RESULTS

Figure 1 shows a comparison between our KMC simulation results for the average monomer and island densities and the corresponding RE results obtained by numerically integrating Eqs. (12)–(14). The KMC results for $D_h/F=10^5, 10^7$, and 10^9 are shown, while the value of R_0 ($R_0=1/3$) was chosen to give the best fit to the KMC data. As can be seen, there is excellent agreement between the RE and KMC results over all coverages and for all values of D_h/F. Thus, as was previously found in two dimensions,[17] the self-consistent RE approach can be used to accurately predict average quantities such as the monomer and island density in three dimensions. We now consider the scaled ISD.

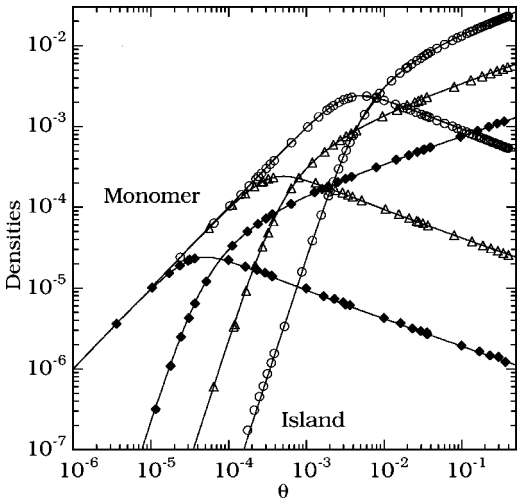

FIG. 1. Comparison between KMC results (symbols) and the corresponding RE results (solid lines) for the monomer density N_1 and island density N as a function of coverage for $D_h/F=10^5$ (circles), 10^7 (triangles), and 10^9 (diamonds).

Figure 2 shows the corresponding results for the scaled ISD obtained from KMC simulations (symbols) at coverage $\theta=0.2$. As can be seen, the peak of the scaled ISD increases with increasing D/F while the island-size distribution becomes sharper, thus indicating a divergence in the asymptotic limit of infinite D/F. Also shown in Fig. 2 are the corresponding self-consistent RE results (solid curves). The asymptotic MF result[12,18] $f(u)=\frac{1}{3}(1-2u/3)^{-1/2}$ correspond-

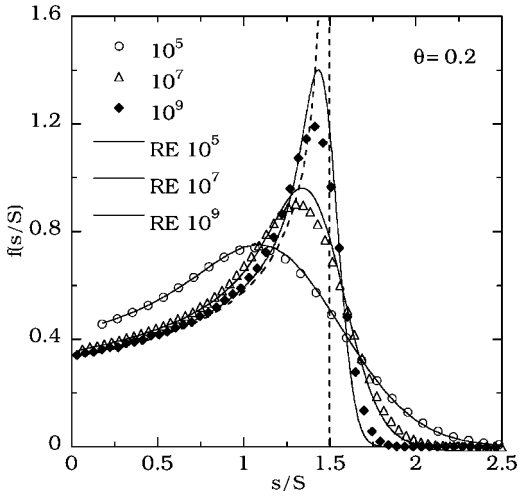

FIG. 2. Scaled island-size distributions for $D_h/F=10^5$, 10^7, and 10^9. KMC simulation results (symbols), RE results (solid lines), and asymptotic MF limit (dashed curve).

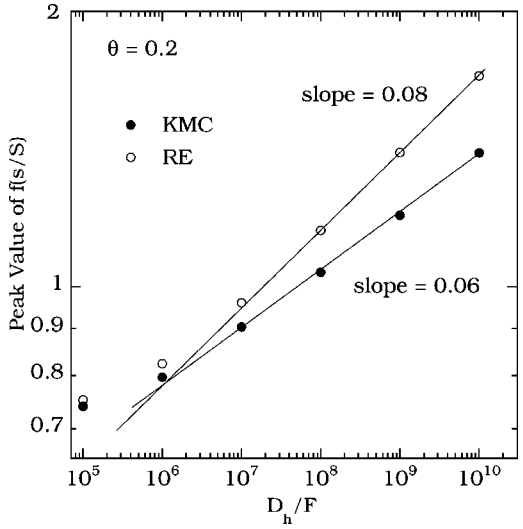

FIG. 3. Log-log plot of peak value of scaled ISD as function of D_h/F.

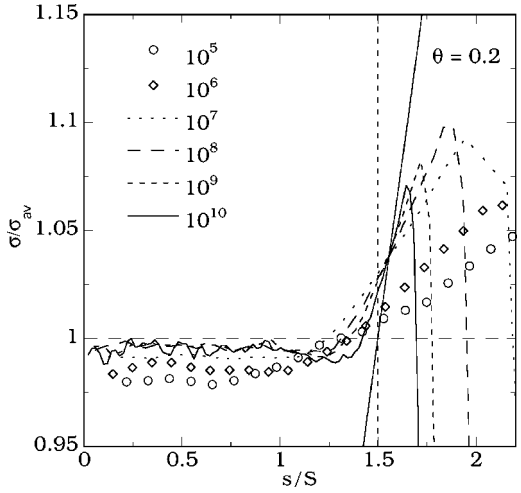

FIG. 4. KMC simulation results for scaled CND σ_s/σ_{av} versus scaled island size for $D_h/F=10^5-10^{10}$. Horizontal dashed line corresponds to MF CND; solid line corresponds to $(2/3)(s/S)$.

ing to infinite D/F is also shown (dashed curve). As expected, the self-consistent MF RE results for the ISD approach the asymptotic MF prediction with increasing D/F. However, there are significant differences between the KMC results and the RE results. In particular, while there is good agreement between the KMC and RE results for small D/F, for large D/F the KMC results for the scaled ISD are significantly lower than the RE predictions.

These differences are more dramatically indicated in Fig. 3 which shows the peak values of the scaled ISD obtained from both KMC simulations and RE calculations as a function of D/F. As can be seen, in both cases the peak value $f_{pk}(D/F)$ of the scaled ISD increases as a power law—i.e., $f_{pk}\sim(D/F)^{\phi}$—thus indicating a divergent ISD in the asymptotic limit. However, the value of ϕ obtained from the KMC simulations ($\phi\simeq 0.06$) is significantly smaller than the value ($\phi\simeq 0.08$) obtained from our RE calculations.

In order to understand these differences, we have also measured the scaled capture-number distribution $C(s/S)$ in our KMC simulations for $D_h/F=10^5-10^{10}$ as shown in Fig. 4. The MF prediction corresponding to the horizontal dashed line $C(u)=1$ is also shown. As can be seen, there are significant deviations between the KMC results and the MF prediction. In particular, $C(u)$ is less than 1 for $u<1.3$ while it increases rapidly with u for $u>1.3$. We note that the MF prediction corresponds to an asymptotic divergence in the scaled ISD at the point $u_c^{MF}=3/2$ where the MF CND crosses the line $2u/3$. On the other hand, for large D/F the scaled CND curves obtained from the KMC simulation appear to "pivot" with increasing D/F around a fixed point at $u_c\simeq 1.55$ which is also the point at which they cross the line $2u/3$.

As indicated by Eq. (4), a divergence in the asymptotic ISD will only occur if $C'(u_c)<2z-1=1/3$. For all values of D/F considered here, the slope $C'(u_c)$ of the scaled CND at the crossing point $u_c\simeq 1.55$ is lower than the critical value $2z-1=1/3$ required to avoid a divergence. Furthermore, for large D/F the slope is well described by the expression $C'(u_c)=(1/3)\exp[-a/(D/F)^{0.2}]$ where $a=23.6$. Thus $C'(u_c)$ is less than the critical value of $1/3$ for all finite D/F although it approaches the critical value asymptotically. These results are consistent with the observed divergence in the scaled ISD with increasing D/F. However, the asymptotic divergence appears to occur at a point, $u_c\simeq 1.55$, which is somewhat beyond the point $u_c^{MF}=3/2$ at which the MF ISD diverges.

In order to better understand the asymptotic behavior we have also studied the dependence of the peak position u_{pk} of the scaled ISD obtained from our KMC simulations as a function of D/F. In order to extrapolate the asymptotic behavior, the peak position $u_{pk}(D/F)$ was fit to the form $u_{pk}(D/F)=u_{pk}(\infty)+c(D/F)^{-\gamma}$ while the value of γ was varied to find the best fit. A similar fit was used to extrapolate the MF RE results. Figure 5 shows the corresponding results for the KMC simulations (solid circles, $\gamma\simeq 1/9$) as well as for

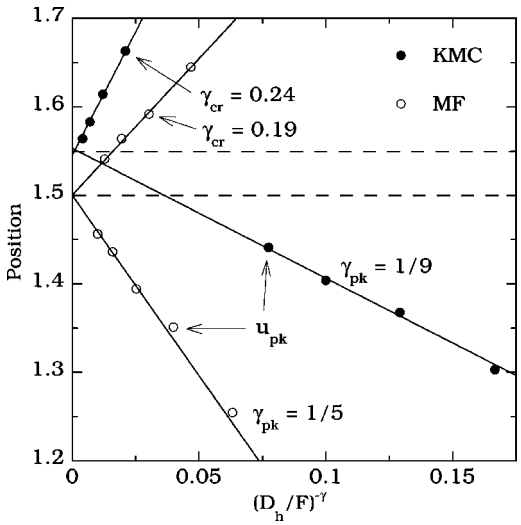

FIG. 5. Plot of $u_{pk}(D/F)$ and $u_{cr}(D/F)$ as a function of $(D_h/F)^{-\gamma}$ for D_h/F ranging from 10^5 to 10^{10}. Lines are fits as described in text while values of γ correspond to best fits.

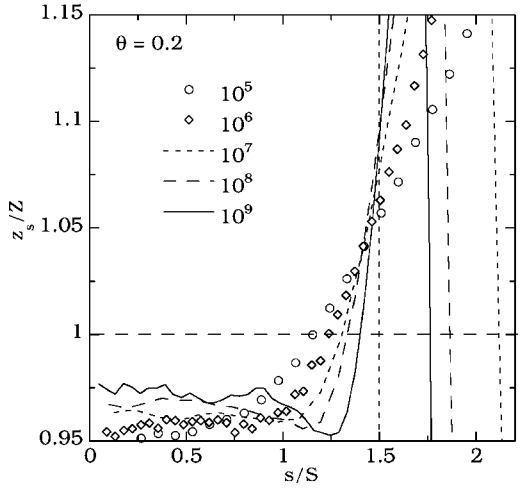

FIG. 6. KMC simulation results for scaled capture zone z_s/Z versus scaled island size s/S for $D_h/F=10^5-10^9$.

the MF RE results (open circles, $\gamma\simeq 1/5$). As expected, for the MF RE results we find $u_{pk}^{MF}(\infty)\simeq 3/2$. However, for the KMC simulation results we find $u_{pk}(\infty)\simeq 1.55$ which is in good agreement with our results for the scaled CND. We note that the value of γ ($\gamma\simeq 1/9$) obtained in our fits to the KMC results may be partially explained by noting that $(D/F)^{1/9}$ corresponds to the ratio of the island separation to the island size. However, we have no similar explanation for the value of γ ($\gamma\simeq 0.20$) obtained in our fits to the MF RE calculations.

We have carried out a similar analysis of the crossing point u_{cr} corresponding to the position at which the tails of successive ISD curves (corresponding to values of D/F varying by a factor of 10) cross. In this case a fit similar to that used for the peak position—i.e., $u_{cr}(D/F)=u_{cr}(\infty)+c(D/F)^{-\gamma}$—was used and again the value of γ was varied to find the best fit. The corresponding results are also shown in Fig. 5. We note that the best-fit value of γ ($\gamma\simeq 0.24$) used for the KMC crossing points (upper solid symbols) is significantly different from that used to fit the scaling of the KMC peak position ($\gamma\simeq 1/9$) and is much closer to that used for the MF RE results (upper open symbols). However, the asymptotic value of the crossing point $u_{cr}(\infty)\simeq 1.55$ is still in good agreement with the asymptotic value for the peak position. Similarly, for the MF RE results we again find $u_{cr}^{MF}(\infty)\simeq 3/2$ and $\gamma\simeq 1/5$. Thus these results confirm that, as already indicated in Figs. 2–4, although the asymptotic scaled ISD diverges with increasing D/F, it is significantly different from the MF prediction.

For completeness, we have also measured the scaled CZD as shown in Fig. 6. The shape of the scaled CZD is similar to that of the scaled CND. In particular, it is relatively "flat" for $u<1.3$, while for $u>1.3$ it increases rapidly with island size for large D/F. However, just as for the case of 2D submonolayer nucleation,[19] the scaled CZD is quite different from the scaled CND. This difference is most likely due to the effects of geometry as well as fluctuations which imply that an adatom in the capture zone of a given island is not necessarily captured by that island.

V. DISCUSSION

In order to understand the role of fluctuations and geometry in irreversible nucleation and growth, and also to compare with results obtained in two dimensions, we have carried out simulations of a simple point-island model of irreversible island nucleation and growth in three dimensions. We have also presented a self-consistent RE calculation similar to that previously carried out by Bales and Chrzan[17] in two dimensions. In contrast to the case of island nucleation and growth in 2D, we find that the peak of the scaled ISD increases and the distribution becomes sharper with increasing D/F, thus leading to a divergence in the asymptotic limit. However, while good agreement is found between the self-consistent RE results for the average island and monomer densities and our simulation results, there is poor agreement between the MF RE results for the scaled ISD and simulations. In particular, the scaled island-size distribution obtained in KMC simulations diverges more slowly than the MF prediction.

By directly measuring the scaled capture-number distribution for different values of D/F we have found that, in contrast to the MF assumption, the scaled CND depends weakly on island size. In addition, our analysis of the dependence of the scaled CND on D/F clearly indicates that the asymptotic CND is also different from the MF prediction. In particular, the asymptotic CND appears to cross the line $2u/3$ at a value $u_c\simeq 1.55$ which is somewhat larger than the MF prediction $u_c=3/2$. As indicated by Eq. (1), this leads to a divergence of the ISD at a value $u_c\simeq 1.55$ which is somewhat larger than the value $3/2$ predicted by MF theory. These results are further supported by our analysis of the asymptotic behavior of the ISD peak position and crossing point which indicate that in both cases there is an asymptotic divergence at a scaled island size $u_c\simeq 1.55$ which is somewhat beyond the MF prediction. This "bending" of the CND away from the MF value $C(u)=1$ for large u also leads to a decreased value of the numerator in Eq. (1), thus explaining the "decrease" in the peak of the ISD compared to the MF prediction. Thus, we conclude that although the scaled ISD and CND in 3D are significantly closer to the MF prediction than in 2D, in the asymptotic limit of large D/F the scaled CND is still not completely independent of island size as predicted by MF theory. We believe that this is due to the effects of fluctuations and geometry, which still appear to play a significant role in 3D.

We note that since we have been primarily interested in the asymptotic behavior of the point-island model, the results shown here have primarily focussed on the behavior at a relatively high coverage—i.e., $\theta=0.2$. While at higher coverages the differences between our KMC results and the MF prediction are even larger, we have also examined the behavior at significantly lower coverage $\theta\simeq 0.05$. In this case, we found that a similar discrepancy between the KMC results and the MF prediction also occurs, although it is significantly smaller for the same value of D/F. We conclude that at lower coverages, much higher values of D/F are needed to clearly see the asymptotic behavior. Finally, we note that for a more realistic model with 3D islands, the dependence of the capture number on island size is likely to be even stron-

ger than for the point-island model studied here. Based on these results, we expect that the "critical dimension" d_c for mean- field behavior for the point-island model is larger than 3 and is possibly equal to 4. In the future we plan to carry out parallel KMC simulations in four dimensions in order to see if this is the case.

ACKNOWLEDGMENTS

This research was supported by the NSF through Grant No. DMR-0219328. We would also like to acknowledge grants of computer time from the Ohio Supercomputer Center (Grant No. PJS0245).

*Electronic address: fengshi@physics.utoledo.edu
†Electronic address: yshim@physics.utoledo.edu
‡Electronic address: jamar@physics.utoledo.edu

[1] J. A. Stroscio and D. T. Pierce, Phys. Rev. B **49**, R8522 (1994).
[2] J. A. Stroscio, D. T. Pierce, and R. A. Dragoset, Phys. Rev. Lett. **70**, 3615 (1994).
[3] H. Brune, H. Roder, C. Boraguo, and K. Kern, Phys. Rev. Lett. **73**, 1955 (1994).
[4] Z. Y. Zhang and M. G. Lagally, Science **276**, 377 (1997).
[5] J.-K. Zuo and J. F. Wendelken, Phys. Rev. Lett. **78**, 2791 (1997).
[6] B. Muller, L. Nedelmann, B. Fischer, H. Brune, J. V. Barth, and K. Kern, Phys. Rev. Lett. **80**, 2642 (1998).
[7] M. Zinke-Allmang, Thin Solid Films **346**, 1 (1999).
[8] B. Fischer, H. Brune, J. V. Barth, A. Fricke, and K. Kern, Phys. Rev. Lett. **82**, 1732 (1999).
[9] I. Furman *et al.*, Phys. Rev. B **62**, R10649 (2000).
[10] R. Ruiz, B. Nichel, N. Koch, L. C. Feldman, R. F. Haglund, A. Kahn, F. Family, and G. Scoles, Phys. Rev. Lett. **91**, 136102 (2003).
[11] J. A. Venables, Philos. Mag. **27**, 697 (1973).
[12] J. A. Venables, G. D. Spiller, and M. Hanbucken, Rep. Prog. Phys. **47**, 399 (1984).
[13] M. C. Bartelt and J. W. Evans, Phys. Rev. B **46**, 12675 (1992).
[14] M. C. Bartelt and J. W. Evans, J. Vac. Sci. Technol. A **12**, 1800 (1994).
[15] J. G. Amar, F. Family, and P. M. Lam, Phys. Rev. B **50**, 8781 (1994).
[16] C. Ratsch, A. Zangwill, P. Smilauer, and D. D. Vvedensky, Phys. Rev. Lett. **72**, 3194 (1994).
[17] G. S. Bales and D. C. Chrzan, Phys. Rev. B **50**, 6057 (1994).
[18] J. G. Amar and F. Family, Phys. Rev. Lett. **74**, 2066 (1995).
[19] M. C. Bartelt and J. W. Evans, Phys. Rev. B **54**, R17359 (1996).
[20] J. A. Blackman and P. A. Mulheran, Phys. Rev. B **54**, 11681 (1996).
[21] P. A. Mulheran and J. A. Blackman, Surf. Sci. **376**, 403 (1997).
[22] P. A. Mulheran and D. A. Robbie, Europhys. Lett. **49**, 617 (2000).
[23] J. G. Amar, M. N. Popescu, and F. Family, Phys. Rev. Lett. **86**, 3092 (2001).
[24] M. N. Popescu, J. G. Amar, and F. Family, Phys. Rev. B **64**, 205404 (2001).
[25] J. G. Amar, M. N. Popescu, and F. Family, Surf. Sci. **491**, 239 (2001).
[26] J. W. Evans and M. C. Bartelt, Phys. Rev. B **63**, 235408 (2001).
[27] J. W. Evans and M. C. Bartelt, Phys. Rev. B **66**, 235410 (2002).
[28] J. A. Venables and H. Brune, Phys. Rev. B **66**, 195404 (2002).
[29] J. G. Amar and M. N. Popescu, Phys. Rev. B **69**, 033401 (2004).
[30] P. A. Mulheran, Europhys. Lett. **63**, 379 (2004).
[31] M. von Smoluchowski, Z. Phys. Chem., Stoechiom. Verwandtschaftsl. **17**, 557 (1916); **92**, 129 (1917).
[32] L. A. Nesbit, Appl. Phys. Lett. **46**, 38 (1994).
[33] Wai Lek Ng *et al.*, Nature (London) **410**, 192 (2001).
[34] T. Fischer *et al.*, Thin Solid Films **276**, 100 (1996).
[35] D. R. S. Talbot and J. R. Willis, Proc. R. Soc. London, Ser. A **370**, 351 (1980).